Using Surface Active Random Copolymers To Control the Domain Orientation in Diblock Copolymer Thin Films

E. Huang and T. P. Russell*

Polymer Science and Engineering Department, Silvio O. Conte National Center for Polymer Research, University of Massachusetts, Amherst, Massachusetts 01003

C. Harrison and P. M. Chaikin

Department of Physics, Princeton University, Princeton, New Jersey 08544

R. A. Register

Department of Chemical Engineering, Princeton University, Princeton, New Jersey 08544

C. J. Hawker

IBM Almaden Research Center, 650 Harry Road, San Jose, California 95120-6099

J. Mays

Department of Chemistry, University of Alabama at Birmingham, Birmingham, Alabama 35294-1240

Received May 4, 1998; Revised Manuscript Received July 10, 1998

ABSTRACT: The structure of thin films of a symmetric diblock copolymer, P(dS-*b*-MMA) (dS = perdeuterated styrene, MMA = methyl methacrylate), was investigated near preferential and nonpreferential (neutral) surfaces. Neutral surfaces were achieved at the substrate and air interfaces by localizing random copolymer, P(S-*r*-MMA), having a styrene fraction of 0.60, to each of these interfaces. This was performed by chemically grafting the random copolymer to the substrate and anchoring a surface active random copolymer having a perfluorinated end group to the air interface, respectively. Neutron reflectivity and small-angle neutron scattering were used to determine the orientation of the lamellar microdomains for films having various boundary conditions. Successive steps of CF_4 reactive ion etching followed by field emission scanning electron microscopy were used to ascertain the orientation of the microdomains as a function of film depth. For films confined between two continuous neutral surfaces, the orientation of the lamellar microdomains is observed to be perpendicular to the film surfaces throughout the entire film thickness.

Introduction

Thin films of diblock copolymers have attracted considerable attention recently due to their potential use as nanolithographic templates[1] for the generation of quantum electronic structures,[2] catalytic surfaces,[3] and separation membranes.[4] Block copolymers are ideally suited for this purpose since films can be prepared easily, the copolymers self-organize into a periodic array of nanostructures, and the shape and size of the domains can be regulated by the relative and total molecular weight of each block, respectively.

The behavior of diblock copolymers in thin films differs from that in the bulk since interfacial interactions control the evolution of their structure.[5,6] For diblock copolymer films composed of cylindrical or lamellar microdomains, interfacial interactions dictate the wetting layers at both the substrate and surface interfaces and, consequently, the orientation of the microdomains in the film. Preferential wetting of either the air or substrate interfaces by one of the blocks leads to a parallel orientation of the microdomain morphology with respect to these interfaces. For films having thicknesses less than the characteristic period, interfacial interactions will dictate the wetting layers at the interfaces, but film thickness constraints may result in a change in the fundamental repeat of the morphology or a change in the morphology itself.[7]

Utilization of these arrays of nanoscopic structures, however, requires control over the spatial orientation of the microdomains. This study focuses on the orientation of the copolymer microdomains normal to the surface. Several approaches have been used to achieve perpendicular orientation of the microdomains. Perpendicular orientation has been observed for metastable films containing either lamellar or cylindrical morphologies by solvent casting procedures.[1] Confinement of the diblock copolymer film to thicknesses that are incommensurate with the domain size has also been predicted to promote a perpendicular microdomain orientation, which has been confirmed experimentally.[8] Finally, perpendicular lamellae have been observed for hybrid liquid crystalline block copolymer thin films[9] and triblock copolymer films.[10]

An alternative approach to achieving a perpendicular orientation of the morphology is to remove or balance all interfacial interactions,[11] i.e., using nonpreferential or neutral surfaces. Interfacial interactions can be controlled by self-assembling mixed monolayers on a surface, as shown by Genzer and Kramer.[12] Kellogg et al.[13] showed that the placement of random copolymers, consisting of the same monomeric units as the diblock copolymer, at the confining surfaces can achieve this end. However, potential diffusion of the random copolymer into the confined diblock layer produced am-

10.1021/ma980705+ CCC: $15.00
Published on Web 10/10/1998

biguities in this work. Recently, Mansky et al.[14] showed that by anchoring brushes of random copolymers of styrene and methyl methacrylate, designated as P(S-*r*-MMA), to silicon substrates, diffusion of the random copolymer away from the interface was arrested while control over interfacial interactions was achieved. By controlling the composition of the random copolymer brush, the interfacial interactions can be changed and at ~60% of styrene, all interactions were balanced; i.e., the interactions of the polystyrene or poly(methyl methacrylate) blocks with the interfaces were equal and the surface is effectively neutral.[15] Mansky et al.[16] further demonstrated the influence of the anchored random copolymers in a study of disordered P(S-*b*-MMA). Their experiments showed a loss of all preferential segregation to the substrate interface when the neutral random copolymer brush was grafted to the substrate. Studies on microphase separated P(S-*b*-MMA) show that lamellar microdomains oriented normal to the substrate interface having the neutral random copolymer brush. At the air surface, however, the lower surface energy of PS induced an alignment of the lamellae parallel to the air surface. The resultant film, therefore, consisted of a mixed morphology having lamellae of perpendicular and parallel orientations.[17]

In this article, a method is described by which both surfaces can be made neutral. It has been shown previously that perfluoroalkyl terminated polymers strongly segregate to a polymer/air interface due to the lower surface energy of fluorinated groups.[18,19] Incorporating this strategy, perfluorodecanoyl moieties were chemically end-linked to random copolymers having compositions identical to the neutral random copolymer brushes described above. The strong segregation of the perfluorodecanoyl terminated random copolymer to the surface effectively traps the diblock copolymer between two random copolymer brushes where the interactions can be controlled. In particular, a simple method is proposed to confine the copolymer film between two neutral walls, which leads to an orientation of the microdomains normal to the surface.

Experimental Section

Synthesis. P(S-*r*-MMA), with a styrene fraction of 0.60 (as determined by NMR) was synthesized in bulk via a TEMPO "living" free radical polymerization using a unimolecular initiator. This provided random copolymers with one hydroxy and one TEMPO terminus. The weight average molecular weight, M_w, and polydispersity, M_w/M_n, was determined to be 9600 and 1.80, respectively, by size exclusion chromatography (SEC). The preparation of the unimolecular initiator and the polymerization of the random copolymer have been described previously.[20−22]

A 1.04 g (~0.19 mmol) sample of the α-hydroxy-ω-TEMPO P(S-*r*-MMA) described above was dissolved in 40 mL of distilled tetrahydrofuran (THF) and heated to 62 °C under a nitrogen purge. A 0.12 mL aliquot (~0.45 mmol) of perfluorodecanoyl chloride (see ref 18), which corresponds to a $2^1/_2$-fold excess, was added to the reaction vessel. The mixture was allowed to react for 20 h, and the reaction vessel was allowed to cool to room temperature. Quantitative yields can be expected due to the facile addition and large excess of the perfluoronated groups. The reaction mixture was passed through a basic alumina column to remove hydrochloric acid and excess perfluorodecanoyl groups. The polymer was then precipitated in methanol.

P(dS-*b*-MMA) was synthesized anionically. The d indicates that the polystyrene block was perdeuterated. SEC results yielded $M_w = 50\,000$ with $M_w/M_n = 1.35$. The morphology was observed to be lamellar with a characteristic period of 360 Å and a dPS volume fraction of 0.53 as determined from solution NMR studies.

Characterization. Neutron reflectivity (NR) and small-angle neutron scattering experiments (SANS) were performed on the NG7 beam guide at the National Institute of Standards and Technology in Gaithersburg, MD. For neutron reflectivity, a wavelength of $\lambda = 4.75$ Å was used with a resolution of $\Delta q_z/q_z = 5\%$, where $q_z = (4\pi/\lambda)\sin\theta$ and θ is the grazing incidence angle. Small-angle scattering was performed using neutrons having a wavelength of $\lambda = 4.75$ Å ($\Delta\lambda/\lambda = 22\%$), a sample aperture diameter of 0.953 cm, and a beam stop diameter of 7.62 cm.

X-ray photoelectron spectroscopy (XPS) results were obtained with a Perkin-Elmer Physical Electronics 5100 spectrometer using Mg Kα (200 W, 15 kV) X-rays. Survey scans which correspond to large binding energy scans and higher resolution sweeps of the C_{1S} region were obtained using pass energies of 89.45 and 39.75 eV, respectively. Atomic sensitivity factors were determined from measurements performed on samples of known compositions: F_{1S}, 1.000; C_{1S}, 0.250; O_{1S}, 0.660. The total exposure of samples to X-rays was kept below 10 min to prevent appreciable degradation to the methyl methacrylate units.

Polymer film etching was performed at the Cornell Nanofabrication Facility (CNF) using a customized reactive ion etcher (RIE) by Applied Materials, Inc. The etching was performed with a CF_4 gas flow rate of 10 cm^3 (STP)/min, a pressure of less than 1 mTorr, and a power density of 0.08 W/cm^2. These etching parameters were chosen because low-power, low-pressure CF_4 based RIE has been shown to smoothly etch block copolymer films at a controllable rate.[23] An etching rate of 150 Å/min was determined by ellipsometry measurements of polymer film thicknesses before and after etching. The measured etching rate reflects an average of the etching rates of both PS and PMMA.

Scanning electron microscope (SEM) images were obtained with a Leo Gemini 982 field emission gun SEM at CNF. To minimize charging, a low incident beam voltage (1−5 kV) was used. Secondary electron signals were collected from both an in-lens and side detector. The lighter regions of the images correspond to ridges of PS left after etching, and the darker regions correspond to troughs of etched away PMMA. Image contrast in nonetched samples results from degradation and removal of the PMMA by the electron beam. Film thicknesses were measured wifh a Rudolph Research ellipsometer using a helium−neon laser ($\lambda = 6328$ Å) at an incidence angle of 70°. IR spectra were obtained with a Bio-Rad spectrometer.

Results and Discussion

Synthesis and Characterization of Surface Active Random Copolymers. Surface active random copolymers were synthesized via an esterification reaction where hydroxy terminated random copolymers were reacted with an excess of perfluorodecanoyl chloride, as shown in Scheme 1. IR spectroscopy confirmed the modification of the random copolymer as the peak attributed to the ester linkage of the perfluorodecanoyl group to the random copolymer is present for the modified polymer. Figure 1 shows the IR spectra in the carbonyl stretching region for the modified and unmodified random copolymers (Figure 1a,b, respectively). The absorption band at 1729 cm^{-1} originates from the methyl methacrylate units, and the small band at 1779 cm^{-1} arises from the ester linkage between the perfluorodecanoyl termination and the random copolymer.[18] As can be seen, the latter peak is only observed for the modified random copolymer.

The surface activity of the modified random copolymers was examined with X-ray photoelectron spectroscopy (XPS). Thin films, ~1000 Å, of the modified random copolymer were spin-coated on to silicon substrates. XPS surveys and C_{1s} regional sweeps were

Scheme 1

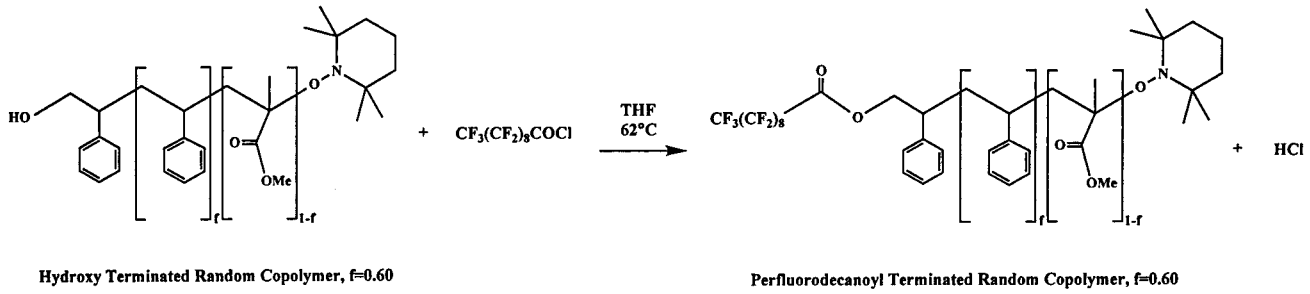

Hydroxy Terminated Random Copolymer, f=0.60

Perfluorodecanoyl Terminated Random Copolymer, f=0.60

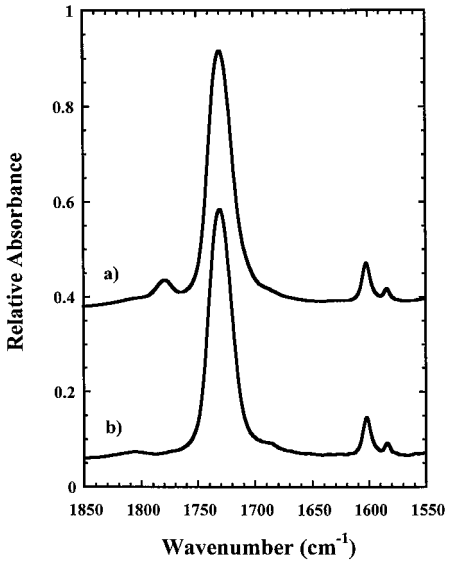

Figure 1. IR spectra of (a) α-perfluorodecanoyl, *ω*-TEMPO P(S-*r*-MMA) and (b) α-hydroxy-*ω*-TEMPO P(S-*r*-MMA). The styrene fraction, *f*, in random copolymer is 0.60.

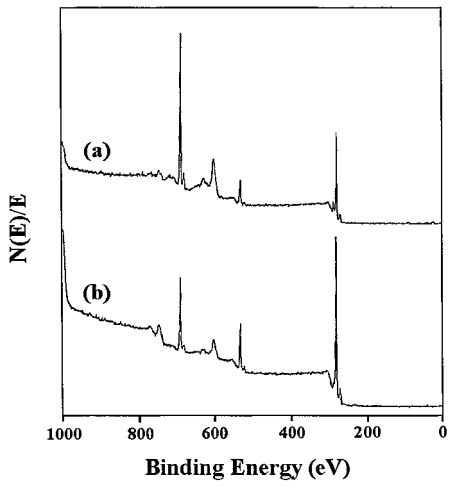

Figure 2. XPS survey of surface active random copolymer film at (a) 15 and (b) 75° takeoff angles.

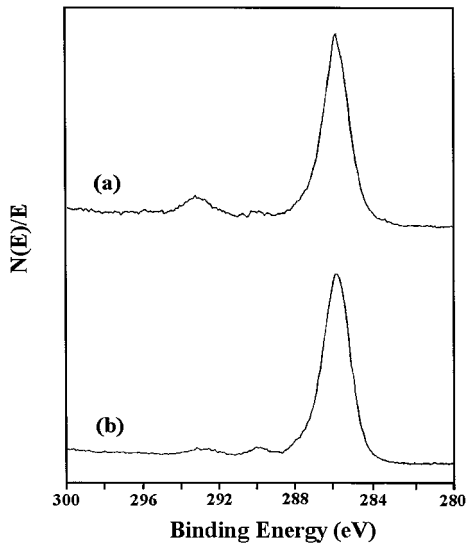

Figure 3. XPS C_{1s} region for surface active random copolymer film at (a) 15 and (b) 75° takeoff angles.

obtained at takeoff angles of 15 and 75° from the sample plane, for samples as-cast and after annealing under vacuum for 17 h at 160 °C. The 15 and 75° takeoff angles correspond to sampling depths of ∼11 and ∼40 Å, respectively (95% of observed photoelectrons originate from these sampling depths). Furthermore, there is an exponential decrease in sensitivity with sampling depth. This effect is significant at higher takeoff angles; e.g., at a 75° takeoff angle, 54% of the observed photoelectrons originate from the uppermost 11 Å.

Figure 2 shows the XPS spectra of the as-cast sample at 15 and 75° takeoff angles. It is observed that the fluorine peak, found at a binding energy of 690 eV, is significantly larger at a 15° takeoff angle. The fluorine peaks obtained at 15 and 75° takeoff angles correspond to atomic percentages of 22.3 and 9.0%, respectively. Figure 3 shows the higher resolution XPS spectra for the C_{1s} at 15 and 75° takeoff angles. Three peaks are observed at binding energies of 293.5, 290, and 286 eV. The peak at 293.5 eV is attributed mainly to carbon atoms attached to fluorine atoms (C−F carbons). Carbon atoms in the phenyl rings of styrene units that undergo a $\pi \rightarrow \pi^*$ transition also contribute to this region, but this contribution is minor. The peaks at 290 and 286 eV correspond to ester carbons and carbons bonded to hydrogen atoms, respectively. From Figure 3, it is evident that the peak at 293.5 eV (C−F peak) is significantly larger at a 15° takeoff angle. Integration of the three carbon peaks provides quantitative information regarding the relative amounts of the different types of carbons observed. A comparison of the C−F peaks at the two takeoff angles shows that carbons bonded to fluorine atoms comprise 7.6 and 2.2% of the total carbon atoms observed for the 15 and 75° takeoff angles, respectively.

These results correspond to an enrichment of fluorine at the surface and indicate that the perfluorodecanoyl groups are segregating to the surface. For this segregation to occur, a layer consisting largely of random copolymer must exist below the layer containing the perfluorodecanoyl groups. Thus, the system adopts a structure where there is a layer of the random copolymer at the air surface with the perfluorodecanoyl groups

Table 1. XPS Results[a]

		atomic %			% of carbon types		
sample	angle (deg)	C	O	F	C1	C2	C3
as-cast	15	67.6	10.1	22.3	7.6	1.0	91.4
	75	78.4	12.6	9.0	2.2	1.5	96.3
annealed	15	63.6	12.0	24.4	7.9	1.4	90.7
	75	76.0	14.2	9.8	2.8	1.8	95.4

[a] C1 corresponds to carbon atoms having C−F bonds. C2 corresponds to carbon atoms having a C=O bond. C3 corresponds to all other carbon atoms.

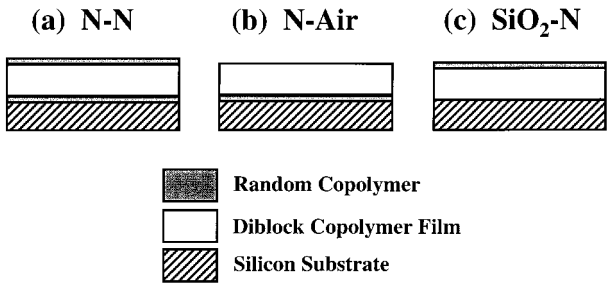

Figure 4. Illustration of the three systems studied: (a) diblock copolymer film confined between two random copolymer brush surfaces, N−N; (b) diblock copolymer film on substrate grafted random copolymer brush without surface active random copolymer, N−Air; (c) diblock copolymer film on silicon substrate with surface active random copolymer applied to polymer/air interface, SiO_2−N.

serving as the anchoring points. The XPS results for the annealed sample were found to be similar to those of the as-cast sample (Table 1), indicating that the segregation occurred during casting.

Effect of Surface Active Random Copolymers on Domain Orientation. The influence of the random copolymer interfaces on the orientation of the copolymer microdomains was examined under three different conditions. These include the following: neutral random copolymer at both interfaces, a neutral random copolymer anchored only to the substrate, and neutral random copolymer anchored only to the air/polymer interface. They are denoted as N−N, N−Air, and SiO_2−N, respectively, and are shown schematically in Figure 4. The thickness of the lamellar diblock copolymer film used in these three systems was held constant at 1700 Å, which is ∼4.7 repeat periods of the lamellar microdomain morphology, L_o, measured to be ∼360 Å.[17] The case of a diblock copolymer film on a silicon substrate with a free surface is not discussed since previous work[24] has shown that the lamellae are oriented parallel to the substrate.

For the N−N and N−Air samples, hydroxy-terminated random copolymers in toluene were spin coated onto 5 mm thick, 5 cm diameter cleaned silicon substrates. The random copolymer thin films (∼600 Å thick) were annealed under vacuum at 160 °C for ∼4 days to ensure complete reaction of the hydroxy termini to the native oxide and then rinsed thoroughly with toluene. The thickness of the resultant random copolymer brushes, determined by optical ellipsometry, was ∼60 Å. The diblock copolymer films were then spin coated from toluene solutions onto two random copolymer brush surfaces and one clean silicon substrate.

A thin film of the surface active polymer having a thickness of ∼60 Å was spin coated from a toluene solution onto a ∼5 × 7.5 cm microscope slide. This thickness corresponds to a single monolayer of the surface active random copolymer. The sides of the microscope slide were scored with a razor blade, and the copolymer film was floated onto a pool of deionized water and was retrieved with the previously coated Si substrates, effectively sandwiching the diblock copolymer film between the substrate and the surface active copolymer.

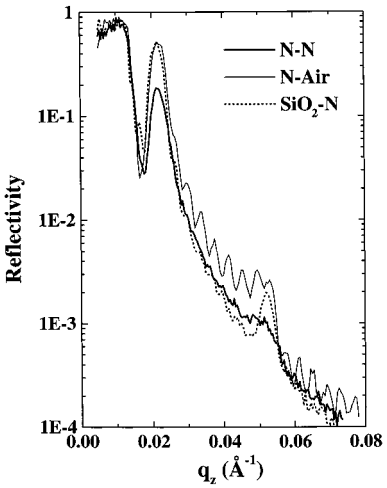

Figure 5. Neutron reflectivity data of N−N, N−Air, and SiO_2−N samples. First-order Bragg reflection is at $q_z = 0.022$ Å^{-1}.

The three samples were annealed under vacuum at 170 °C for 26 h. The neutron reflectivity profiles of each of the specimens are shown in Figure 5. Neutron reflectivity profiles of ordered symmetric diblock copolymer films typically show Bragg peaks characteristic of the lamellar repeat period normal to the substrate and Kiessig fringes that result from the total film thickness. A Bragg peak was observed at $q_z = 0.022$ Å^{-1} ($q_z = (4\pi/\lambda) \sin\theta$, where λ is the wavelength and θ is the incidence angle) for each of the samples, indicating that some parallel orientation of the lamellae existed in each of the samples. As can be seen, however, the intensities of the Bragg peak differed greatly between the three samples, indicating significant differences in the amount of ordering parallel to the surface. The N−N, N−Air, and SiO_2−N samples had maximum peak reflectivities of 0.187, 0.517, and 0.523, respectively. For the two samples that had the random copolymer floated onto the surface, the Kiessig fringes are small and not well-resolved due, most likely, to the surface roughnesses produced in transferring a very thin film of low molecular weight polymer by the floating method.

Small-angle neutron scattering experiments were performed as a function of the incident angles, where the incident angle is defined as the angle between the surface plane and the neutron beam. It has been shown previously that small-angle neutron scattering can be extended to thin polymeric films.[17,25] Two-dimensional scattering contours obtained at incident angles of 90° (normal to the substrate) and 30°, are shown in Figure 6 for the three samples. For each of the samples at 90° incidence, an isotropic scattering ring is observed. In this geometry, density correlations parallel to the surface are probed. The presence of a scattering ring indicates that there are lamellae oriented normal to the surface. The intensity of the maximum, proportional to the total number of lamellae oriented normal to the surface, is greatest for the N−N case. At 30° incidence, meridonal arcs are observed for the N−N and N−Air cases, arising from lamellae oriented normal to the surface and parallel to the neutron beam.

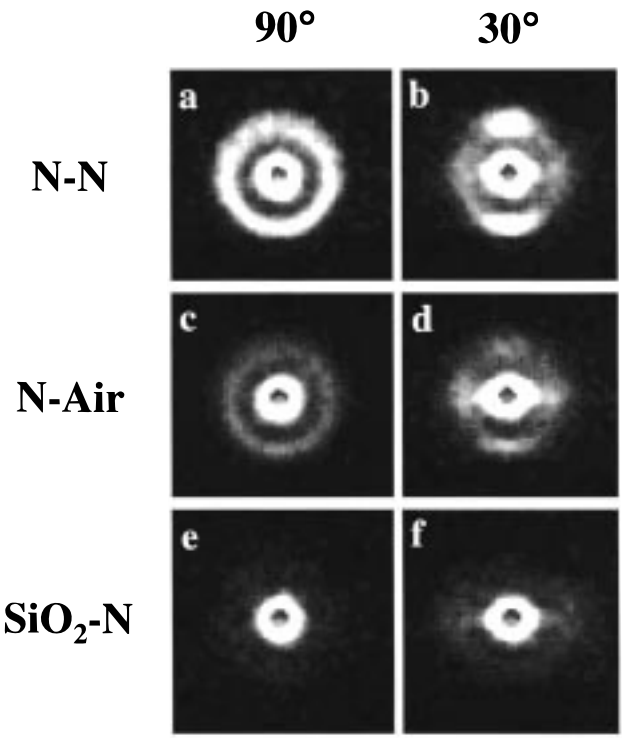

Figure 6. Small-angle neutron scattering patterns of (a) N−N at a 90° tilt angle, (b) N−N at a 30° tilt angle, (c) N−Air at a 90° tilt angle, (d) N−Air at a 30° tilt angle, (e) SiO_2−N at a 90° tilt angle, and (f) SiO_2−N at a 30° tilt angle. The vertical direction on the scattering patterns at 30° tilt corresponds to the tilt axis.

The NR and SANS data show that the amount of perpendicular orientation is highest when the diblock copolymer film is confined between two neutral random copolymer surfaces. For the N−N case, the Bragg peak in the NR profile is the weakest and SANS intensities, for the ring and meridonal arcs at tilt angles of 90° and 30°, respectively, are the strongest. The amount of normal orientation is considerably less for the N−Air sample, as expected, since the preferential wetting of the dPS block at the air surface promotes a parallel orientation of the lamellae at the air surface. Interestingly, the number of lamellae oriented normal to the surfaces is negligible for the SiO_2−N sample. The difference between the N−Air and SiO_2−N cases can be attributed to the strength of the interactions at the interfaces. In the N−Air, the strongest driver for parallel alignment is only the difference in surface energies between PS and PMMA. This is relatively small. In the SiO_2−N case, however, strong interactions between the PMMA block and the native oxide layer is sufficiently strong to outweigh any effect of the neutral interface.

Orientation of Lamellae as a Function of Film Depth. To further assess the orientation of the lamellae in the film, real space images were obtained as a function of depth. A relatively new technique was used where the film surface was imaged with a field emission scanning electron microscope, FESEM, after the removal of part of the film.[23] Here, the film is exposed to a carbon tetrafluoride, CF_4, reactive ion etch that etches into the surface of the polymer. The amount of polymer film removed can be controlled by the exposure time. Successive etching steps followed by imaging with the FESEM provide information regarding the morphology and its orientation as a function of film depth. It should be noted that CF_4 etchant is chosen over oxygen plasma etching as the latter leads to significant increases in roughness. With CF_4, the etching rate of PMMA is approximately three times that of PS. For lamellae perpendicular to the substrate this produces a roughness characteristic of the morphology that permits a means by which once can distinguish the PMMA regions from the PS regions. FESEM imaging can be performed with the contrast provided by the topography formed from the etching process, and no staining is required.

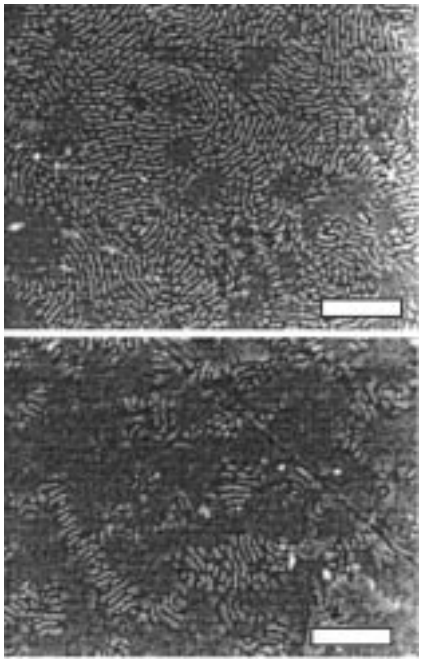

Figure 7. FESEM images taken at two different locations from the N−N sample prior to etching. The amount of perpendicular lamellae near the surface is not uniform over the sample surface. The contrast is due to topography induced by the degradation of PMMA in the electron beam. The bars represent 500 nm.

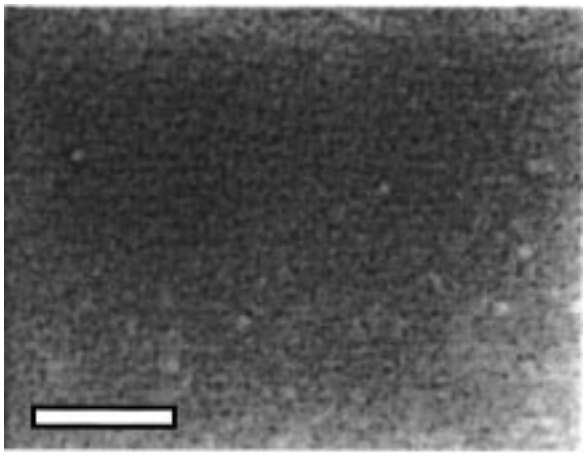

Figure 8. FESEM image from the N−Air sample prior to etching. No perpendicular lamellae were observed. The bar represents 500 nm.

FESEM images of the samples studied by NR and SANS prior to etching are shown in Figures 7 and 8. The contrast shown in these images arises from height differences caused by the electron beam degradation of PMMA. For the N−N sample (Figure 7), perpendicular lamellae were observed, but the coverage was nonuniform in that some regions exhibited a high concentration

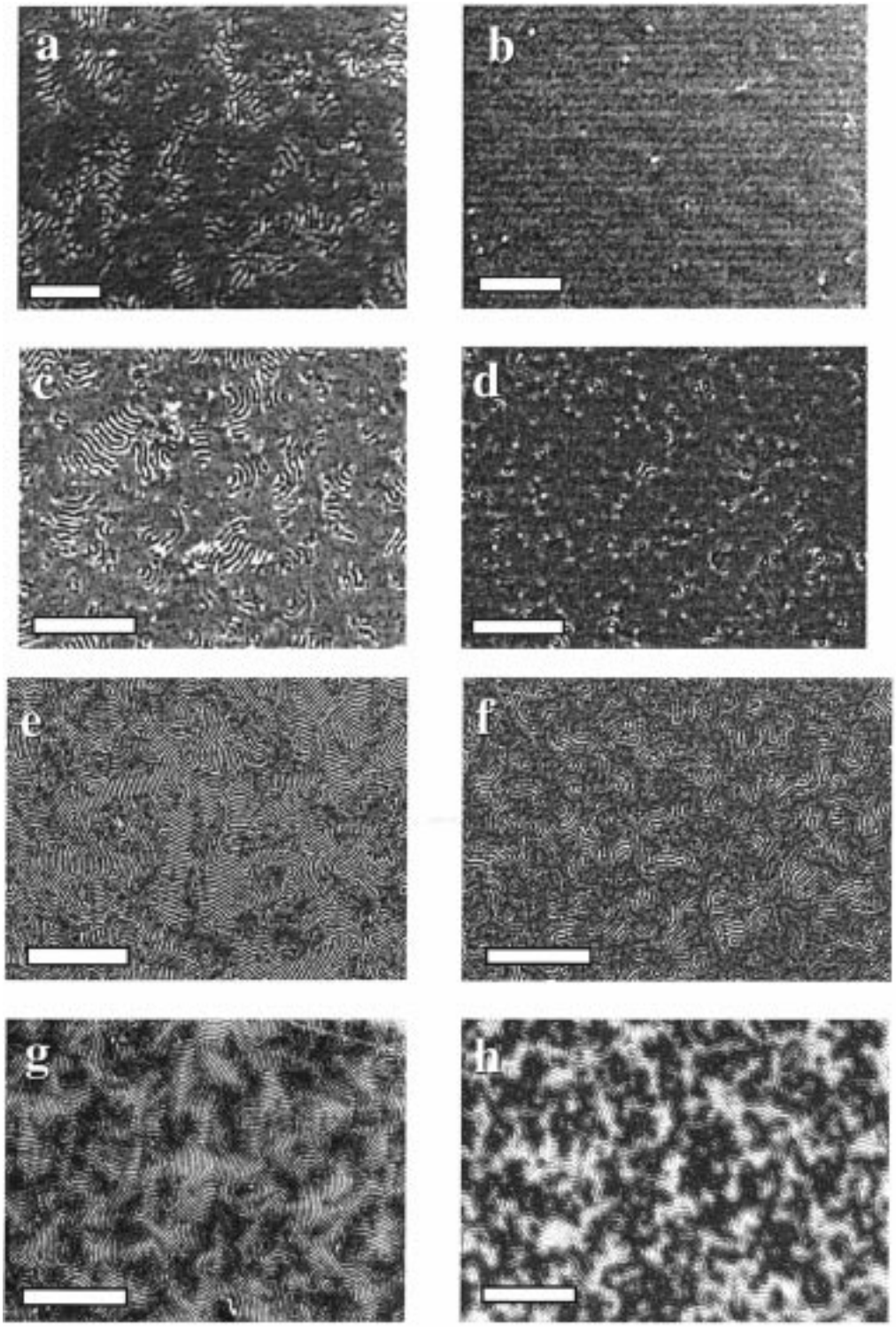

Figure 9. FESEM images taken from: (a) N−N and (b) N−Air samples after ∼230 Å of the film was etched away; (c) N−N and (d) N−Air samples after ∼600 Å of the film was etched away; (e) N−N and (f) N−Air samples after ∼1200 Å of the film was etched away; and (g) N−N and (h) N−Air samples after ∼1450 Å of the film was etched away. The bars represent 500 nm in a and b and 1 μm in c−h.

of perpendicular lamellae while others showed less. No perpendicular lamellae were seen at the surface for the N−Air case, as would be expected (Figure 8). Finally, the SiO_2−N sample surface predominantly showed parallel lamellae, though small areas (∼1% of the film surface) of perpendicular lamellae were observed.

The N−N and N−Air samples were then successively etched to depths of approximately 230, 600, 1200, and 1450 Å and imaged with FESEM. Typical topographies are shown in Figure 9. A comparison between the two films shows that perpendicular lamellae are present throughout the entire N−N film and are not appreciably observed in the N−Air sample until approximately 600 Å of the film is removed. At an etch depth of 1200 Å the N−N samples show perpendicular lamellae with grains square micrometers in size. The amount of perpendicular lamellae in the N−Air sample is less, and the lamellar order persists only over small distances.

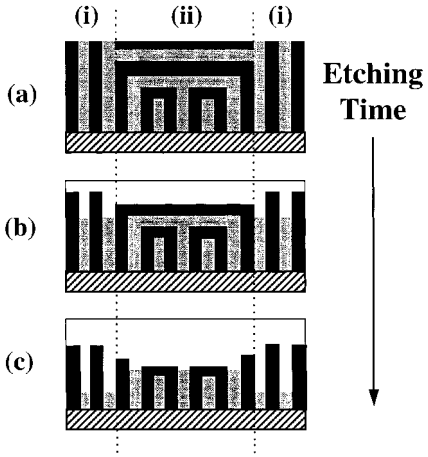

Figure 10. Schematic of topography generated at different etching depths: (a) no etch, (b) moderate etch, and (c) deep etch. Region i corresponds to regions having only perpendicular lamellae. Region ii corresponds to regions having parallel lamellae on top of perpendicular lamellae. Rectangular outlines in b and c represent initial film thicknesses. dPS and PMMA domains are shown in black and gray, respectively. Note that PMMA domains etch approximately three times faster than dPS domains.

Finally, at etching depths of 1450 Å, with ~250 Å of copolymer remaining, a strong normal orientation of the lamellar microdomains is seen for both samples.

Examination of the micrographs at etch depths of 1200 and 1450 Å shows a mottling of the image on the 0.5 μm size scale; i.e., brighter and darker areas are evident on this size scale. This mottling is more evident at greater etch depths. The texture can be attributed to areas where lamellae are oriented parallel to the surface. To understand this, one can use the schematic diagrams shown in Figure 10. As the ion beam etches through the sample, areas where the lamellar orientation is different will etch differently. In areas where the lamellae are normal to the surface, the etching will be dictated by the etching rate of the PS microdomains. However, in areas where there is a parallel alignment of the lamellae, the etching rate will be dictated by a combination of the etching rate of PS and PMMA. Since PMMA etches more rapidly, areas with parallel alignment will etch more rapidly and, consequently, will appear darker.

Evolution of Lamellar Ordering. To study the ordering process of diblock copolymers between two neutral surfaces, NR and SANS experiments were performed on five different samples, each having thicknesses of ~1370 Å, that were confined between two neutral surfaces. These samples were annealed under vacuum at 170 °C for different times, quenched to room temperature (well below T_g), and, subsequently, examined with NR and SANS. To ensure a uniform and rapid heat transfer to the samples, the sample substrates were placed on a large, thermally equilibrated, aluminum block under vacuum for a specified period of time and then quenched to room temperature prior to measurement. Three of the samples were returned to the vacuum oven, annealed further, and remeasured.

The time dependence of the neutron reflectivity profiles is shown in Figure 11. With no annealing, no sign of parallel ordering of the lamellae is evident. After 15 min of annealing, a change in the reflectivity near $q_z \sim 0.025$ Å^{-1} is evident. With increasing time, a maximum at $q_z \sim 0.022$ Å^{-1} is seen to intensify,

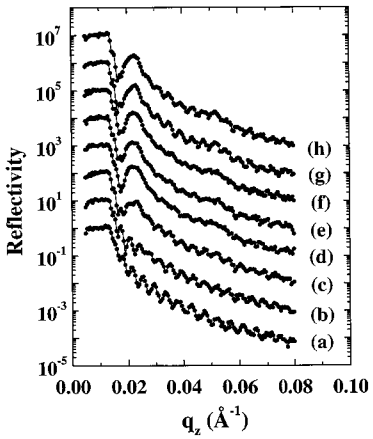

Figure 11. Neutron reflectivity data as a function of annealing time at 170 °C for a sample confined between two neutral surfaces. The data correspond to the following annnealing times: (a) 0 h; (b) 15 min; (c) 1 h; (d) 3 h; (e) 6.75 h; (f) 13.25 h; (g) 24 h; (h) 40 h. The data are offset for clarity.

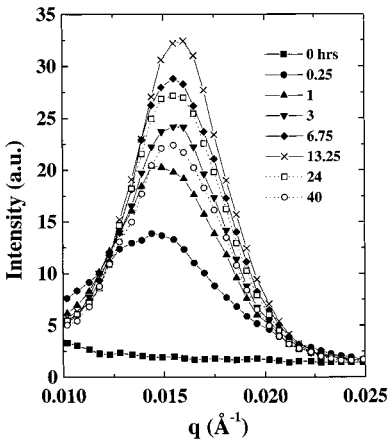

Figure 12. SANS scattering profiles as a function of annealing time for a sample confined between two neutral surfaces.

indicative of an increasing number of lamellae or the enhanced ordering of lamellae parallel to the surface. Even at long times, the maximum peak intensity is only ~0.153, indicating that the number of lamellae oriented parallel to the surface is small. The initial growth of this maximum is slow.

Shown in Figure 12 is the corresponding SANS profiles as a function of time. At time 0, there are no strong correlations in the neutron scattering length density parallel to the surface. After 15 min a strong maximum at 0.0144 Å^{-1} is evident. With increasing time, the maximum is seen to shift toward slightly higher scattering vectors and increase in intensity. After 13 h the intensity of this peak reaches a maximum value and then begins to decrease, suggesting that the orientation of the lamellae normal to the surface is quite rapid. With time, i.e., at 24 and 40 h, the number of lamellae parallel to the surface increases at the expense of lamellae oriented normal to the surface, as seen by the reduction in the SANS peak intensity. The decrease in the number of lamellae oriented normal to the surface observed at longer annealing times may be attributed to the lack of registry between the lamellae growing from the two surfaces or imperfections in the surface active random copolymer films floated onto the surface. The combined NR and SANS results unequivocally show that the neutral surfaces induce a rapid alignment of the lamellae normal to the surface.

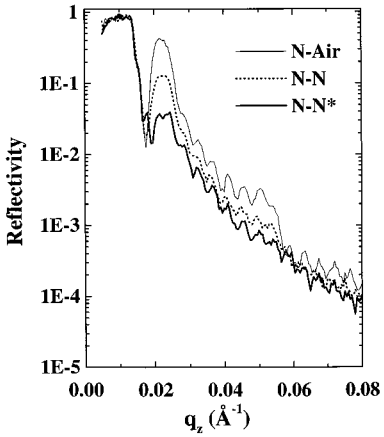

Figure 13. Neutron reflectivity data comparing three samples: N−N* sample where surface active random copolymer layer was spin coated on from acetic acid solution, N−N sample where surface active random copolymer layer was floated on, and N−Air sample. Diblock copolymer film thicknesses in each of these films are approximately 1400 Å.

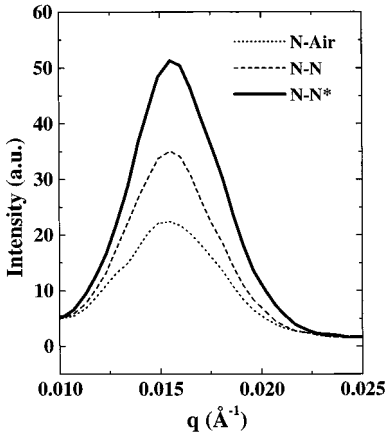

Figure 14. Small-angle neutron scattering data comparing three samples: N−N* sample where surface active random copolymer layer was spin coated on from acetic acid solution, N−N sample where surface active random copolymer layer was floated on, and N−Air sample. Diblock copolymer film thicknesses in each of these films are approximately 1400 Å.

Effect of Casting of Surface Active Random Copolymer. Although the results involving the confinement between two neutral surfaces clearly show the presence of perpendicular lamellae throughout the thickness of the film, there is still a considerable amount of the parallel orientation. This may be attributable to nonuniformities of the surface active random copolymer film floated onto the surface. Since the molecular weight of this random copolymer is low and the film thickness is small (∼60 Å), the mechanical properties of the film are poor. This causes substantial cracking of the film and a loss of integrity of the floated film. This, in turn, leaves areas where the copolymer is not covered and is exposed to air. This will result in areas where there is a preference for parallel alignment of the lamellae. Other routes of applying the surface active random copolymer were, therefore, explored to provide a more uniform layer and to facilitate the processing. It was found that the surface active random copolymer was soluble in acetic acid while the diblock copolymer was not. Therefore, it was possible to spin coat the surface active random copolymer film directly onto the diblock copolymer film without disturbing the structure of the underlying film.

The ramifications of this slight change in the deposition of the surface active random copolymer on the orientation of the lamellar microdomains are profound. To demonstrate this, results on three different samples will be discussed. In all cases a diblock copolymer was spin coated onto a Si substrate to which a neutral random copolymer brush was anchored. The first sample was left exposed to air (designated N−Air); with the second sample, the surface active copolymer was floated onto the diblock copolymer (designated as N−N); and for the third, the surface active random copolymer was spin coated onto the surface of the block copolymer (designated as N−N*).

Neutron reflectivity data from these samples after annealing at 170 °C for 40 h are shown in Figure 13. The N−Air, N−N, and N−N* samples had maximum Bragg peak reflectivities of 0.400, 0.13, and 0.039, respectively. Thus, by casting the surface active random copolymer from acetic acid, the Bragg reflection is suppressed by an order of magnitude as compared to the N−Air sample and is one-third that of the N−N sample. This shows that the number of lamellae oriented parallel to the surface is markedly lower for the sample having the surface active random copolymer which was spin coated onto the surface from an acetic acid solution.

SANS results for the same samples are shown in Figure 14. In these data, the intensity of the interference maximum is nearly 70% greater for the N−N* sample than for the N−N and nearly five times greater than that for the N−Air sample. Since both the peak position and the full width at half-maximum are the same for each sample, the relative increase in the peak intensity is directly related to the number of lamellae oriented normal to the surface. Consequently, NR and SANS results clearly show a pronounced enhancement in the orientation of the lamellae normal to the substrate surface. FESEM provides additional direct evidence to support this. Shown in Figure 15 a−c are the FESEM results for the N−N* sample at different etching depths. Though the contrast in the image is poor, the surface is covered with lamellae oriented normal to the surface. As the sample is etched, the orientation of the lamellae normal to the surface is preserved at all depths.

Conclusions

The combined NR, SANS, and FESEM studies presented here demonstrate that the orientation of copolymer microdomains can be controlled by manipulating the interfacial interactions of the copolymer. In particular, by removing preferential affinities of the copolymer segments with the interfaces, the microdomain morphology of the copolymer can be forced to assume an orientation normal to the substrate interface. Eliminating preferential interactions at both the substrate and surface interfaces leads to the case where the microdomain orientation normal to the surface persists through the entire film. In this work, control over the interfacial interactions was achieved by use of random copolymers where the interactions can be easily and precisely manipulated by changing the composition of the random copolymer. At the substrate, anchoring the copolymer to the substrate prevents diffusion of the random copolymer away from the substrate. At the air

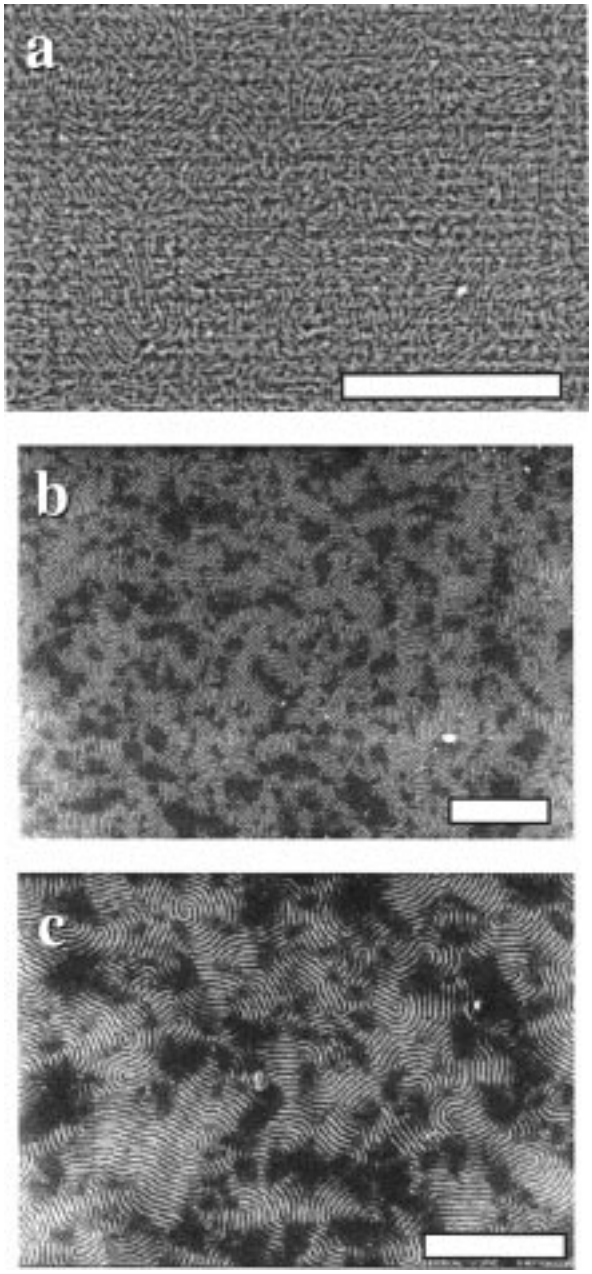

Figure 15. FESEM image of N−N* sample with (a) no etch, (b) 200 Å of film etched away, and (c) 520 Å of film etched away. The bars represent 1 μm.

surface, a block copolymer comprised of a perfluorodecanoyl block and a random copolymer block was used where the low surface energy of the perfluorodecanoyl block effectively anchored this copolymer to the air surface, thereby confining the diblock copolymer of P(S-*b*-MMA) between two neutral surfaces. It was also shown that a uniform coverage of the surface active random copolymer was essential in order to generate a laterally uniform morphology. The methods presented in this article are simple and quite robust and are applicable to other systems. Film thickness effects have not been treated in this article though; for neutral surfaces, this should not be a critical factor.

Acknowledgment. The authors wish to acknowledge Drs. L. Sung and S. K. Satija for assistance with the neutron reflectivity measurements and Dr. S. Kline for assistance with SANS. We are particularly indebted to Drs. Z. Su and T. J. McCarthy for providing purified perfluorodecanoyl chloride and for their useful discussions. We would also like to express our thanks to Dr. M. Park for assistance with the reactive ion etching. This work was supported by the Office of Basic Energy Sciences (Grant DE-FG02-96ER45) and the National Science Foundation through the Materials Research Science and Engineering Center at the University of Massachusetts (Grant DMR-9400488) and the Princeton Center for Complex Materials (Grant DMR-9400362).

References and Notes

(1) Mansky, P.; Chaikin, P.; Thomas, E. *J. Mater. Sci.* **1985**, *30*, 1987.
(2) McEuen, P. L. *Science* **1997**, *278*, 1729.
(3) Mercier, L.; Pinnavaia, T. J. *Adv. Mater.* **1997**, *9*, 500.
(4) Martin, C. R. *Science* **1994**, *266*, 1961.
(5) Fredrickson, G. H. *Macromolecules* **1987**, *20*, 2535. Henkee, C.; Thomas, E. L.; Fetters, L. *J. Mater. Sci.* **1988**, *23*, 1685. Anastasiadis, S. H.; Russell, T. P.; Satija, S. K.; Majkrzak, C. F. *Phys. Rev. Lett.* **1989**, *62*, 1852. Russell, T. P.; Coulon, G.; Deline, V. R.; Miller, D. C. *Macromolecules* **1989**, *22*, 4600. Liu, Y.; Zhao, W.; Zheng, X.; King, A.; Singh, A.; Rafailovich, M. H.; Sokolov, J. *Macromolecules* **1994**, *27*, 4000. Brown, G.; Chakrabarti, A. *J. Chem. Phys.* **1994**, *101*, 3310.
(6) Mayes, A. M.; Russell, T. P.; Bassereau, P.; Baker, S. M.; Smith, G. S. *Macromolecules* **1994**, *27*, 749. Russell, T. P.; Mayes, A. M.; Kunz, M. S. In *Ordering in Macromolecular Systems*; Springer-Verlag: Berlin, Heidelberg, 1994; pp 217−223.
(7) Spatz, J. P.; Moller, M.; Noeske, M.; Behm, R. J.; Pietralla, M. *Macromolecules* **1997**, *30*, 3874−3880. Fasolka, M. J.; Harris, D. J.; Mayes, A. M. *Phys. Rev. Lett.* **1997**, *79*, 3018. Morkved, T. L.; Jaeger, H. M. *Europhys. Lett.* **1997**, *40*, 643.
(8) Walton, D. G.; Kellogg, G. J.; Mayes, A. M.; Lambooy, P.; Russell, T. P. *Macromolecules* **1994**, *27*, 6225. Kikuchi, M.; Binder, K. *J. Chem. Phys.* **1994**, *101*, 3367. Brown, G.; Chakrabarti, A. *J. Chem. Phys.* **1995**, *102*, 1440. Pickett, G.; Balazs, A. C. *Macromolecules* **1997**, *30*, 3097. Matsen, M. W. *J. Chem. Phys.* **1997**, *106*, 7781.
(9) Wong, G. C. L.; Commandeur, J.; Fischer, H.; Jeu, W. H. d. *Phys. Rev. Lett.* **1996**, *77*, 5221.
(10) Stocker, W.; Beckmann, J.; Stadler, R.; Rabe, J. *Macromolecules* **1996**, *29*, 7502.
(11) Pickett, G. T.; Witten, T. A.; Nagel, S. R. *Macromolecules* **1993**, *26*, 3194.
(12) Genzer, J.; Kramer, E. J. *Phys. Rev. Lett.* **1997**, *78*, 4946.
(13) Kellogg, G. J.; Walton, D. G.; Mayes, A. M.; Lambooy, P.; Russell, T. P.; Gallagher, P. D.; Satija, S. K. *Phys. Rev. Lett.* **1996**, *76*, 2503.
(14) Mansky, P.; Liu, Y.; Huang, E.; Russell, T. P.; Hawker, C. *Science* **1997**, *275*, 1458.
(15) In refs 14 and 16−17, the neutral composition was described to have a styrene fraction of 0.57 ± 0.05. The styrene fraction of the neutral random copolymer in these publications was based on monomer feed compositions. The composition of the neutral random copolymer reported in this paper reflects the actual styrene composition in the polymer as determined by ^{1}H NMR.
(16) Mansky, P.; Russell, T. P.; Hawker, C. J.; Mays, J.; Cook, D. C.; Satija, S. K. *Phys. Rev. Lett.* **1997**, *79*, 237.
(17) Mansky, P.; Russell, T. P.; Hawker, C. J.; Pitsikalis, M.; Mays, J. *Macromolecules* **1997**, *30*, 6810.
(18) Su, Z.; Wu, D.; Hsu, S. L.; McCarthy, T. J. *Macromolecules* **1997**, *30*, 840.
(19) Hunt, J., M. O.; Belu, A. M.; Linton, R. W.; Desimone, J. M. *Macromolecules* **1993**, *26*, 4854. Affrossman, S.; Hartshorne, M.; Kiff, T.; Pethrick, R. A.; Richards, R. W. *Macromolecules* **1994**, *27*, 1588. Elman, J. F.; Johs, B. D.; Long, T. E.; Koberstein, J. T. *Macromolecules* **1994**, *27*, 5341. Iyengar, D. R.; Perutz, S. M.; Dai, C.-A.; Ober, C. K.; Kramer, E. J. *Macromolecules* **1996**, *29*, 1229. Schaub, T. F.; Kellogg, G. J.; Mayes, A. M.; Kulasekere, R.; F., A. J.; H., K. *Macromolecules* **1996**, *29*, 3982. Affrossman, S.; Bertrand, P.; Harshorne, M.; Kiff, T.; Leonard, D.; Pethrick, R. A.; Richards, R. W. *Macromolecules* **1996**, *29*, 4332.

(20) Hawker, C. J. *J. Am. Chem. Soc.* **1994**, *116*, 11314.
(21) Hawker, C. J.; Barclay, G. G.; Orellana, A.; Dao, J.; Devonport, W. *Macromolecules* **1996**, *29*, 5245.
(22) Hawker, C. J.; Elce, E.; Dao, J.; Volksen, W.; Russell, T. P.; Barclay, G. G. *Macromolecules* **1996**, *29*, 2686.
(23) Harrison, C.; Park, M.; Chaikin, P. M.; Register, R. A.; Adamson, D. H.; Yao, N. *Polymer*, **1998**, *39*, 2733. Harrison, C.; Park, M.; Chaikin, P. M., Register, R. A.; Adamson, D. H.; Yao, N. *Macromolecules*, in press.
(24) Coulon, G.; Deline, V. R.; Green, P. F.; Russell, T. P. *Macromolecules*, **1989**, *22*, 2589. Anastasiadis, S. H.; Russell, T. P.; Satija, S. K.; Majkrzak, C. F. *Phys. Rev. Lett*. **1989**, *62*, 1852.
(25) Russell, T. P.; Lambooy, P.; Barker, J. G.; Gallagher, P.; Satija, S. K.; Kellogg, G. J.; Mayers, A. M. *Macromolecules* **1995**, *28*, 787.

MA980705+